THE JOURNAL OF PHYSICAL CHEMISTRY C

Article

pubs.acs.org/JPCC

Monolayer Formation of Molybdenum Carbonyl on Cu(111) Revealed by Scanning Tunneling Microscopy and Density Functional Theory

Peter Krüger,[†] Mikhail Petukhov,*[,†] Bruno Domenichini,[†] András Berkó,[‡] and Sylvie Bourgeois[†]

[†]ICB, UMR 6303 CNRS-University of Burgundy, F-21078 Dijon, France

[‡]Reaction Kinetics Laboratory, INC, CRC of the HAS, University of Szeged, Szeged, Hungary

ABSTRACT: Molybdenum carbonyl $Mo(CO)_6$ was adsorbed on the Cu(111) surface at 160 K in the monolayer coverage range and studied by scanning tunneling microscopy. A well-ordered monolayer of hexacarbonyl molecules was observed experimentally for the first time. The monolayer has a hexagonal structure compatible with a $(\sqrt{7} \times \sqrt{7})R19$ superlattice on the copper (111) plane. The arrangement and orientation of the molecules on the surface were determined by density functional theory calculations, including van der Waals interactions. The comparison of adsorption and cohesive energies reveals that the molecule−substrate interaction is stronger than the intermolecular one, which explains the observed two-dimensional growth.

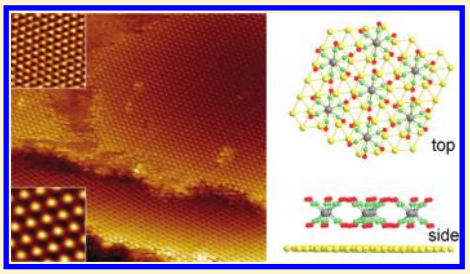

1. INTRODUCTION

Metal carbonyls are a class of organometallic complexes that has a large application potential in nanotechnology. The interest is based on chemical and physical properties of the d-metal compounds: the particular arrangement of π and σ orbitals of the metal carbonyl molecule does not lead to a charge redistribution between the metal and carbon monoxide ligands, and the metal atom stays neutral if one or more of the carbon monoxide groups are lost.[1] This nature of the metal−ligand bond makes the carbonyl molecule unstable under various physical processes, such as thermal activation,[2−4] light irradiation,[5−7] or bombardment with charged particles,[8,9] whereby the molecule's decomposition results in clusters of metal atoms and desorbing carbon monoxide. The fact that the majority of metal carbonyls sublimate at relatively low temperature and can decompose under photon and electron beam irradiation makes these compounds attractive for thin-film deposition and nanofabrication.

One of the potential applications is the lithography by photoirradiation or electron beam exposition in vacuum conditions, where the desired pattern of metal clusters at the micro- and nanoscale can be created by controlled decomposition of metal carbonyl vapor above a substrate.[10,11] Such a technique of electron beam decomposition of $W(CO)_6$ precursor gas performed on the top of a scanning near-optical field microscope (SNOM) cantilever allows one to create a metal whisker, further used as an atomic force microscopy (AFM) tip to obtain simultaneously SNOM and AFM images of the investigated surface.[12] Further, the nanolithography technique could be developed by applying a scanning tunneling microscope attempting to decompose locally the metal carbonyl vapor above a substrate surface by voltage pulses on the tip.[13] As a scanning tunneling microscope (STM) allows a tip positioning on the atomic level, it might give atomic-scale information on the mechanism of decomposition and realize a controlled atom-by-atom cluster growth. For the development of such STM applications for nanolithography by metal carbonyl decomposition, it is important to study the adsorption and film growth of metal carbonyl molecules on appropriate substrates.

Metal carbonyl molecules interact through van der Waals forces and form molecular crystals in bulk. It is interesting to study an arrangement of weakly interacting molecules in a two-dimensional layer on a noble metal substrate. However, structural studies are difficult to perform using standard techniques, such as X-ray photoelectron diffraction (XPD) and low-energy electron diffraction (LEED), because the carbonyl molecules easily decompose under X-ray and electron beam irradiation, as it was mentioned above. In this paper, we report a detailed study of an adsorbed monolayer structure of molybdenum hexacarbonyl molecules on the surface of Cu(111) by STM and first-principles calculations.

2. EXPERIMENTAL AND COMPUTATIONAL DETAILS

The experiment was done in an ultra-high-vacuum (UHV) chamber with a base pressure lower than 1×10^{-10} mbar equipped with a variable-temperature STM (Omicron Nano-Technology). The clean surface of the Cu(111) crystal (Surface Preparation Laboratory, The Netherlands) was prepared by cycles of argon ion-sputtering (0.8 keV, 15 min), followed by annealing at 700 K. The cleaning cycles were repeated until a sharp 1×1 LEED pattern of Cu(111) was observed. The well-defined 1×1 order and the cleanliness of the surface were confirmed by STM with atomic resolution at room temperature and at 160 K achieved by liquid nitrogen cooling.

Received: January 25, 2012
Revised: April 27, 2012
Published: April 30, 2012

STM images were taken using etched Pt/Ir tips. The tips were cleaned by ion-sputtering (Ar^+, 0.8 keV) and annealed in a vacuum at 600 K. When tip shape effects appeared during the work, interfering with the images, the tip shape was corrected by negative voltage pulses (2−4 V) above the clean Cu surface and/or by mildly touching the surface with the tip. The following conditions were used for the STM images: bias voltage, V_b = 5−300 mV; tunneling current, I_t = 1−100 pA for the carbonyl monolayer and 1−20 nA for the clean copper surface with atomic resolution.

The desorption temperature of $Mo(CO)_6$ molecules on most noble metals, metal oxide, and relatively inert surfaces, such as graphite, is around 200 K.[5,8,14] For the Cu(111) substrate, a desorption temperature of 198 K was measured by temperature-programmed desorption.[5] Therefore, the copper crystal was cooled to 160 K and exposed to carbonyl vapor on the STM stage.

$Mo(CO)_6$ powder was placed into a glass tube and mounted to the STM chamber through a leak valve. The tube was covered by aluminum foil in order to prevent a partial decomposition of the molecules due to light irradiation. The powder was turbo-pumped during 10 min just before exposition in order to reduce the partial pressure of carbon monoxide produced by decomposition. Otherwise, carbon monoxide may poison the substrate, preventing adsorption of the carbonyl molecules directly on copper.

The adsorption of the $Mo(CO)_6$ monolayer on Cu(111) is modeled using first-principles calculations based on density functional theory with dispersion force corrections (DFT-D), as proposed by Grimme.[15] The plane-wave code VASP is used with projector-augmented wave potentials as provided in the package and the PBE-GGA exchange-correlation functional.[16,17] The Kohn−Sham orbitals are expanded in plane waves up to 400 eV. The cutoff radius for the dispersion interactions is set to 15 Å. The Cu(111) substrate is modeled with a slab of four monolayers. The lower two monolayers are frozen in their bulk position, and the upper two are free to relax. Repeated Cu slabs are separated by 21.3 Å of vacuum. Once the $Mo(CO)_6$ molecules are adsorbed, the vacuum space between the molecules and the next Cu slab is still more than 12 Å in all cases. To model single molecule adsorption, we place one $Mo(CO)_6$ molecule in a 4 × 4 supercell of Cu(111), with a lateral size of 10.11 Å. The Brillouin zone is sampled with a Γ-centered 3 × 3 ×1 mesh. For the $Mo(CO)_6$ monolayer, both free-standing and adsorbed on Cu(111), we use a $\sqrt{7} \times \sqrt{7}$ R19 supercell with a lateral size of 6.68 Å and k-points on a 6 × 6 × 2 mesh. Except for the results shown in Figure 3, all atomic coordinates of the molecules are fully optimized.

3. RESULTS AND DISCUSSION

The lattice parameter and orientation of the clean copper surface obtained from the STM image (see inset in Figure 1) are used as a reference to determine the monolayer arrangement. The measured values of 2.6 Å for the lateral atom ordering and 2.1 Å for the single step height on the clean surface of the copper crystal are in good agreement with literature values (a_{Cu} = 2.56 Å).[18] Single carbonyl molecules could not be visualized by STM in the temperature range of the experiment (~160 K) because of their high mobility under the tip. This indicates weak bonding of the molybdenum carbonyl to the copper surface atoms, which can be easily perturbed by the temperature factor and/or tip−molecule interaction. After 1−2 L of carbonyl exposition, a uniformly ordered monolayer is formed on terraces of the cooled Cu(111) surface; see Figure 1. The monolayer has a hexagonal structure with a measured lattice parameter of a_{MoCO} = 6.7 Å (±0.1) and axes rotated by about 20° with respect to those of Cu(111). The observed apparent height of the monolayer is about 1 Å, and the corrugation is 0.4 Å. Both the lattice parameter and the orientation of the monolayer are consistent with a commensurate $(\sqrt{7} \times \sqrt{7})$R19 superstructure. This structure is not due to carbon monoxide contamination. CO/Cu(111) system has been quite extensively studied by LEED, and different superstructures have been found depending on the temperature.[19] At the temperature of the substrate T = 160 K, CO forms a $(\sqrt{3} \times \sqrt{3})$R30 structure, as we have checked in separate experiments. The possibility that the observed monolayer is formed by metallic Mo can also be ruled out because of the low surface mobility of Mo atoms at the experimental temperature and the tendency of Mo to form clusters on noble metal substrates.[2]

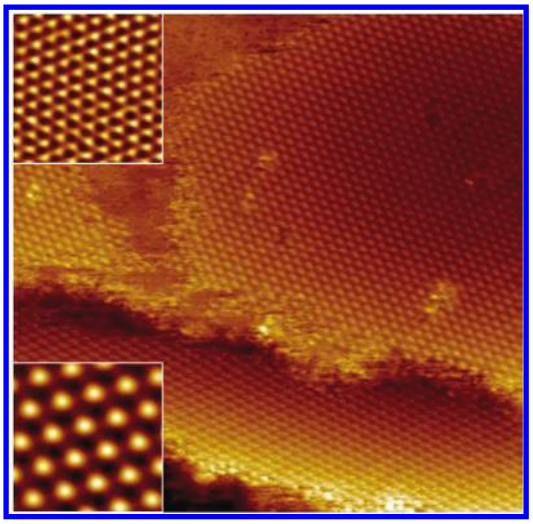

Figure 1. 330 × 330 Å^2 STM image of $Mo(CO)_6$ monolayer on two terraces of Cu(111): tunneling current, I_t = 8 pA; bias voltage, V_b = 300 mV. Upper inset: 24 × 24 Å^2 image of initial Cu(111) surface, I_t = 3 nA, V_b = 10 mV. Lower inset: 24 × 24 Å^2 area of adsorbed carbonyl molecules, I_t = 12 pA, V_b = 300 mV.

Interestingly, scanning of the adsorbed monolayer under bias voltages and tunneling currents higher than V_b = 100−300 mV and I_t = 0.1−1 nA (varying for different tips) usually destroys the monolayer ordering. Indeed, an increased bias voltage and tunneling current excites locally the molecules by a moderate electric field and tip−surface interaction. Under such conditions, the scan produces a disordered striped image, indicating an interaction of molecules with the tip. This shows that already moderate values of the bias voltages and tunneling currents give rise to a tip−surface interaction that is larger than forces holding the molecules in the ordered monolayer structure. However, the monolayer destruction by the scanning tip at a moderate bias voltage can be a result of hexacarbonyl molecule decomposition by the tip at applied tunneling conditions.

The measured lattice parameter of the monolayer (6.7 Å) is comparable with the molecular distances in bulk $Mo(CO)_6$, which has an approximately closed-packed structure where each molecule has 12 nearest neighbors, 6 of which are at distances of 6.48−6.53 Å, and the other 6 at 7.20−7.26 Å.[20] The fact that the nearest-neighbor distance in the monolayer is slightly larger

dx.doi.org/10.1021/jp300832a | J. Phys. Chem. C 2012, 116, 10617−10622

than that in the bulk could be a consequence of the different orientation of the molecules in the monolayer and/or stronger interaction of hexacarbonyl molecules with the substrate in comparison with the intermolecular forces. To understand the molecular orientation in the monolayer, it is useful to compare the measured monolayer unit cell with the molecular dimensions. The size of the $Mo(CO)_6$ molecule is known from the theoretical and experimental bond length data.[21,22] The Mo−O distance is 3.2 Å, which leads to a distance of 4.5 Å between two nearest oxygen atoms in the molecule and 6.4 Å between opposite oxygen atoms; see Figure 2. Three oxygen

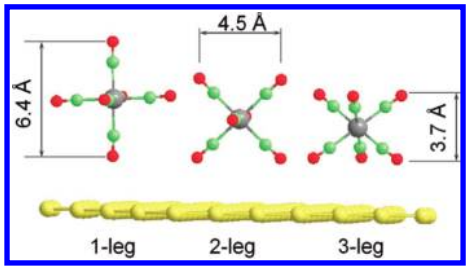

Figure 2. Different $Mo(CO)_6$ molecule orientations with respect to the surface of Cu(111). Gray balls, molybdenum atoms; green balls, carbon atoms; red balls, oxygen; yellow balls, copper.

atoms of CO groups from two opposite sides form two parallel planes with a distance of 3.7 Å between them. There are three high symmetry orientations of the molecule on the surface with the surface normal along the 4-fold, 2-fold, or 3-fold symmetry axis of the molecule (Figure 2). In the following, they are denoted as 1-leg, 2-leg, and 3-leg orientations, respectively.

We carried out first-principles calculations using the DFT-D approach to understand the molecular adsorption and monolayer growth. To check the performance of this approach with respect to the intermolecular forces, we started by studying bulk $Mo(CO)_6$. The optimized lattice constants (a = 11.93 Å; b = 11.29 Å; c = 6.41 Å) agree within about 1% with experiment (a = 12.02 Å; b = 11.42 Å; c = 6.49 Å).[20] The cohesive energy of bulk $Mo(CO)_6$ (defined as the total energy of the bulk minus the energy of free molecules) is E_{coh}(bulk) = −0.58 eV/molecule, which compares favorably with the experimental sublimation enthalpy of −0.73 eV/molecule.[23] It is worth noticing that DFT without dispersion corrections fails to reproduce the structure and energetics of the bulk $Mo(CO)_6$ crystal. With the pure GGA-PBE functional, the average lattice parameter in the bulk is overestimated by 8% and the cohesive energy (−0.13 eV) is by a factor of 5 too small in comparison with the sublimation enthalpy. With the LDA functional, on the other hand, the cohesive energy (−0.62 eV) agrees with experiment, but the lattice constants are underestimated by 4−5%. Also for bulk Cu, the DFT-D scheme performs well with a calculated lattice constant of 3.573 Å, which is only about 1% smaller than the experimental value 3.62 Å.

The Cu(111) substrate was modeled with a slab of four atomic layers, the upper two of which were relaxed. First, the adsorption of a single $Mo(CO)_6$ molecule on Cu(111) was studied in a 4 × 4 surface supercell (10.11 × 10.11 Å^2). We have checked that this cell is large enough that the direct interaction between a molecule and its periodic images becomes negligible. The three principal adsorption orientations shown in Figure 2 have been compared. The optimized distance between the lowest O atom(s) of the molecule and the Cu surface layer is 3.00 (±0.05) Å for all three orientations. Any displacements of the molecule parallel to the surface and rotations around the molecular axis along the surface normal resulted in very small energy variations of 0.01 eV or less. Since the variation is of the same order as the estimated numerical error of the calculations, the exact ground-state adsorption site could not be determined. However, the value 0.01 eV provides a rough estimation of the potential barriers for lateral and rotational diffusion of the molecules on the surface. Such low diffusion barriers correspond to an extremely high mobility of the individual adsorbed molecules, which favors the formation of well-ordered two-dimensional structures at the temperature of the experiment (160 K) and causes the difficulty in observing isolated molecules by STM.

The adsorption energy of a single molecule (SM) is defined as $E_{ads}(SM) = E_{SM/sub} - E_{SM} - E_{sub}$, where $E_{SM/sub}$, E_{SM}, and E_{sub} are the total energies of the adsorbed single molecule, the free single molecule, and the clean metal substrate, respectively.[24] The calculated values of the adsorption energy for the single molecule in the three orientations are given in Table 1. They are in the 0.2−0.5 eV range, which is typical for

Table 1. Calculated Values of Adsorption Energy of a Single Molecule on the Cu(111), E_{ads}(SM); Cohesive Energy of Free Molybdenum Carbonyl Monolayer, E_{coh}; and Energy of $Mo(CO)_6$ Monolayer Formation on the Copper(111) Substrate, E_{form}

molecule orientation	E_{ads}(SM) (eV)	E_{coh} (eV)	E_{form} (eV)
1-leg	−0.21	+0.20	
2-leg	−0.35	−0.01	
3-leg	−0.44	−0.31	−0.71

physisorption. The 3-leg orientation of the single molecule is the most stable configuration with the adsorption energy of −0.44 eV, followed by the 2-leg (−0.35 eV) and 1-leg (−0.21 eV) orientations.

Insight into the nature of the molecule−substrate interaction can be obtained by a density of electronic states (DOS) analysis. The DOS of the hexacarbonyl molecule on the copper surface is shown in Figure 3, curve a. The difference between this DOS and that of the Cu(111) is shown in Figure 3, curve b. The DOS of free molecule is shown in Figure 3, curve c, for comparison. It can be seen that the molecular orbital structure of the molybdenum hexacarbonyl molecule remains unperturbed after adsorption on the copper surface. This shows that

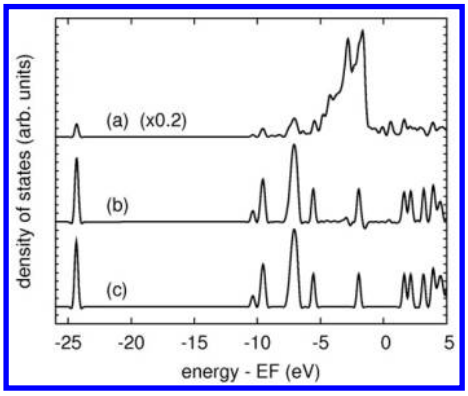

Figure 3. Density of electronic states (DOS): (a) the molecule on the substrate, (b) the difference of the molecule on the substrate and the clean substrate, and (c) the free molecule.

dx.doi.org/10.1021/jp300832a | J. Phys. Chem. C 2012, 116, 10617−10622

there is no covalent bonding between the molecule and the substrate, confirming the mechanism of physisorption. An important observation is that the highest occupied molecular orbitals (at −2.0 eV) and the lowest unoccupied molecular orbitals (at 1.7 eV) are relatively far from the Fermi level. This fact, together with the instability of the monolayer under scanning at increased bias voltages, makes it impossible to image the molecular orbitals. As a consequence, the orientation of the molecules could not be determined from the STM images.

After having discussed the interaction between a single molecule and the substrate, we now turn to the intermolecular interaction within the monolayer. First, we have considered a free-standing hexagonal monolayer of $Mo(CO)_6$ with a lattice constant of 6.684 Å, which is the theoretical value of the $(\sqrt{7} \times \sqrt{7})$R19 superstructure on Cu(111). The system was relaxed without symmetry constraints and starting configurations corresponding to 1-, 2-, and 3-leg orientations of the molecules (Figure 2). The structural optimization was stopped when the total energy converged to 10^{-5} eV. The cohesive energy of the free monolayer per molecule E_{coh} characterizing the lateral intermolecular interaction in different molecular orientations is defined as the difference between the energy of the free monolayer E_{ML} and the energy of the free single molecule E_{SM}: $E_{coh} = E_{ML} - E_{SM}$ (see Table 1). A negative cohesive energy means that a formation of the molecular monolayer is favorable with respect to free molecules. As it can be seen from Table 1, only the monolayer with 3-leg oriented molecules is clearly stable with a substantial cohesive energy of −0.31 eV. When the molecules have the 2-leg orientation, the free molecular layer is only marginally stable ($E_{coh} \approx 0$ eV), and it is unstable with 1-leg-oriented molecules. We have thus clearly established that the 3-leg orientation is the energetically most favorable one with respect to both the molecule−substrate interaction and the molecule−molecule interaction within the monolayer.

It is interesting to note that, in the 1-leg and 2-leg cases, the molecules show appreciable distortion with some Mo−C−O bond angles deviating from the free molecule case up to 10°. In the case of the free monolayer with the 3-leg orientation, in contrast, the molecules are completely undistorted: the difference of atomic positions between the single molecule and the molecule in the monolayer is below numerical precision (<0.01 Å). Note that also, in the bulk crystal, $Mo(CO)_6$ molecules do not show any significant distortion.[20,25] Distortion of the molecules is observed in the calculations whenever an O−O distance between two neighboring molecules is less than about 3 Å, that is, close to twice the van der Waals radius of an oxygen atom (1.342 Å).[15] When the O−O distance is decreased below this distance, Pauli repulsion sets in and provokes the distortion of the molecule and an increase of energy.

The relative stability of the different molecular orientations (1-, 2-, and 3-leg) can be qualitatively understood from simple geometrical arguments and the fact that O−O distances below 3 Å between neighboring molecules are strongly destabilizing. We consider a free hexagonal monolayer with a = 6.684 Å consisting of undistorted molecules in an exact (e.g., untilted) 1-, 2-, or 3-leg orientation. Under these conditions, the only degree of freedom is the azimuthal rotation of the molecules around their symmetry axis normal to the monolayer, described by an azimuthal angle. As a function of azimuthal rotation, the shortest O−O distance between two molecules varies in the following ranges: 0.24−1.73 Å (1-leg), 2.13−2.36 Å (2-leg), and 2.13−3.56 Å (3-leg). Therefore, for 1- and 2-leg orientations, short O−O distances below 3 Å cannot be avoided, which explains the instability of these structures. For the 3-leg orientation, however, the azimuthal angle can be chosen in such a way that "short" O−O distances are absent. Figure 4a,b shows two arrangements corresponding to φ = 0°

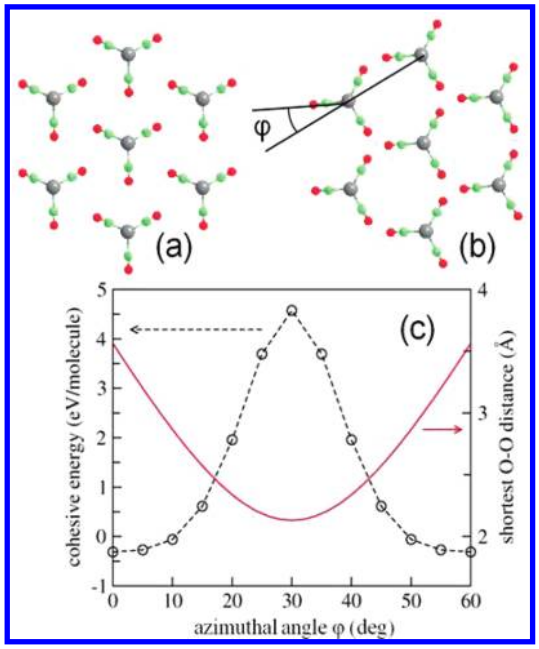

Figure 4. Two arrangements of the free monolayer with 3-leg oriented molecules having different angular dispositions (only three C−O groups of each molecule with oxygen atoms in the same plane are shown for clarity): (a) azimuthal angle φ = 0°; (b) φ is equal to 30°; (c) cohesive energy dependence on azimuthal angle φ (circles and dashed line) and shortest distance of oxygen−oxygen atoms of neighboring molecules as a function of φ.

and φ = 30°. The shortest O−O distance d_{O-O} as a function of φ is plotted in Figure 4c (solid line). The distance exceeds 3 Å only in a small interval of angles around φ = 0° (or multiples of 60°). The calculated cohesive energy of the monolayer E_{coh} with undistorted 3-leg oriented molecules is shown on the same graph (circles and dashed line). The cohesive energy is clearly correlated with d_{O-O}: E_{coh} increases when d_{O-O} decreases, and E_{coh} is negative only when d_{O-O} exceeds a critical value of about 2.5 Å. Qualitatively, the same behavior is found when molecular distortion is taken into account. The fully relaxed structures of the most (φ = 0°) and least (φ = 30°) stable orientations are shown in Figure 4a,b, respectively. The structure in (b) is higher in energy by 0.42 eV than that in (a) and shows considerable distortion of the molecules such that the shortest O−O distance is increased from 2.1 to 2.8 Å.

For the free monolayer in the most stable arrangement (3-leg with φ = 0°) and undistorted molecules, we have studied the cohesive energy as a function of lattice constant. The energy reaches a minimum (−0.34 eV) at a lattice constant of 6.4 Å, which is only slightly below the value of the $(\sqrt{7} \times \sqrt{7})$R19 superstructure ($a_{MoCO}$ = 6.7 Å, with E_{coh} = −0.31 eV). This shows that, even if the molecule−substrate interaction was vanishing, a hexagonal $Mo(CO)_6$ monolayer would have a lattice constant close to the observed one.

Finally, the adsorbed monolayer on Cu(111) was calculated for the 3-leg orientation. A 4 ML Cu(111) slab with the $(\sqrt{7} \times$

dx.doi.org/10.1021/jp300832a | J. Phys. Chem. C 2012, 116, 10617−10622

$\sqrt{7}$)R19 superstructure of molecules was used. Three adsorption sites were considered: Mo on top of the Cu atom, at the hollow site, and the bridge position. The optimized structure for the on-top site of the molybdenum atom is shown in Figure 5. It can be seen that the molecules have the same

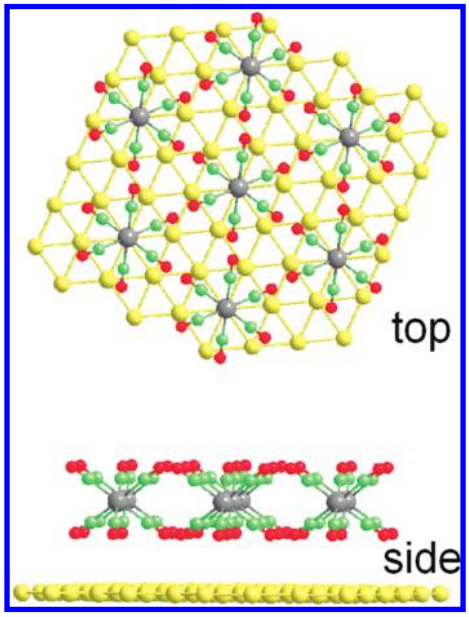

Figure 5. Top and side views of the monolayer structure from first-principles calculations; the molybdenum atom of the molecule is in the on-top position above the copper atom of the surface (yellow balls, cooper atoms; gray balls, molybdenum atoms; green balls, carbon atoms; and red balls, oxygen atoms).

arrangement as in the stable free monolayer. One of the main symmetry axes (O−C)−Mo−(C−O) projected on the surface plane forms an angle of $\varphi = 0°$ with the lattice vectors of the monolayer and thus an angle of 19° with the axes of the Cu(111) substrate. The optimal distance between the three lower O atoms and the Cu surface plane is 3.1 Å. The formation energy of the adsorbed monolayer per molecule is defined as $E_{form} = E_{ML/sub} - E_{ML} - E_{sub}$, where $E_{ML/sub}$ is the total energy of the monolayer on the substrate. The calculated value of energy for monolayer formation is −0.71 eV (Table 1). For on-top, hollow, and bridge adsorption sites, the adsorbed monolayer relaxed to the same molecular orientation and arrangement as the stable free monolayer ($\varphi = 0°$). Within the estimated accuracy of 0.01 eV, the adsorption energy was found to be the same for all three adsorption sites. Therefore, if a definitive adsorption site exists, it could not be determined from the calculation. For purely pairwise interactions, the formation energy would be the sum of the adsorption energy of a single molecule (−0.31 eV) and the formation energy of the free monolayer (−0.44 eV). The fact that the calculated value (−0.71 eV) is close to this sum (−0.75 eV) indicates that the intermolecular and molecule−substrate interactions are indeed essentially pairwise, as expected for van der Waals forces. The calculated formation energy of the adsorbed monolayer is significantly larger in absolute value than the cohesive energy of bulk $Mo(CO)_6$ (−0.58 eV). Consequently, the adsorbed monolayer is stable with respect to cluster formation, in agreement with observation of 2D monolayer growth.

4. CONCLUSIONS

The adsorption of molybdenum hexacarbonyl on the Cu(111) surface has been studied by STM experiments and DFT calculations. At a temperature of 160 K, the $Mo(CO)_6$ molecules adsorb and form a hexagonal monolayer with a measured lattice constant of 6.7 ± 0.1 Å, consistent with a ($\sqrt{7} \times \sqrt{7}$)R19 superstructure on Cu(111). The molecules interact weakly with each other and the copper substrate, indicating van der Waals forces. These have been accounted for in the calculations through the DFT-D scheme. The observed two-dimensional growth is due to the fact that the carbonyl molecules interact more strongly with the substrate than with each other. The calculations show that the molecules in the monolayer have a 3-fold orientation and that neighboring hexacarbonyl molecules avoid short oxygen−oxygen distances.

AUTHOR INFORMATION

Corresponding Author

*Tel: +33-380396155. Fax: +33-380393819. E-mail: Mikhail.Petukhov@u-bourgogne.fr.

Notes

The authors declare no competing financial interest.

ACKNOWLEDGMENTS

This work was supported by the French-Hungarian Intergovernmental S&T Program (FR-18/2008 TÉT).

REFERENCES

(1) Beach, N. A.; Gray, H. B. *J. Am. Chem. Soc.* **1968**, *90*, 5713−5721.
(2) Song, Z.; Cai, T.; Rodriguez, J. A.; Hrbek, J.; Chan, A. S. Y.; Friend, C. F. *J. Phys. Chem. B* **2003**, *107*, 1036−1043.
(3) Evans, J.; Hayden, B. E.; Lu, G. *J. Chem. Soc., Faraday Trans.* **1996**, *92*, 4733−4737.
(4) Cho, S. L.; Bernasek, C. C. *J. Appl. Phys.* **1989**, *65*, 3035−3043.
(5) Ying, Z. C.; Ho, W. *J. Chem. Phys.* **1990**, *93*, 9077−9088.
(6) Ganske, J.; Rosenfeld, R. N. *J. Phys. Chem.* **1989**, *93*, 1959−1963.
(7) Zanoni, R.; Piancastelli, M. N.; McKinley, J.; Magaritondo, G. *Appl. Phys. Lett.* **1989**, *55*, 1020−1022.
(8) So, S. K.; Ho, W. *J. Chem. Phys.* **1991**, *95*, 656−671.
(9) Wang, Y.; Gao, F.; Kaltchev, M.; Tysoe, W. T. *J. Mol. Catal. A: Chem.* **2004**, *209*, 135−144.
(10) Väterlein, P.; Wüstenhagen, V.; Umbach, E. *Appl. Phys. Lett.* **1995**, *66*, 2200−2202.
(11) Walz, M.-M.; Schirmer, M.; Vollnhals, F.; Lukasczyk, T.; Steinrück, H.-P.; Marbach, H. *Angew. Chem., Int. Ed.* **2010**, *49*, 4669−4673.
(12) Chang, W.-S.; Bauerdick, S.; Jeong, M. S. *Ultramicroscopy* **2008**, *108*, 1070−1075.
(13) Majzik, Z.; Balázs, N.; Robin, L.; Petukhov, M.; Domenichini, B.; Bourgeois, S.; Berkó, A. *Vacuum* **2012**, *86*, 623−626.
(14) Yeh, C.-C.; Lai, Y.-H.; Chu, W.-Y.; Yeh, C.-T.; Hung, W. H. *Surf. Sci.* **2004**, *565*, 81−88.
(15) Grimme, S. *J. Comput. Chem.* **2006**, *27*, 1787−1799.
(16) Kresse, G.; Furthmüller, J. *Phys. Rev. B* **1996**, *54*, 11169−11186.
(17) Kresse, G.; Joubert, D. *Phys. Rev. B* **1999**, *59*, 1758−1775.
(18) Huff, W. R. A.; Chen, Y.; Kellar, S. A.; Moler, E. J.; Hussain, Z.; Huang, Z. Q.; Zheng, Y.; Shirley, D. A. *Phys. Rev. B* **1997**, *56*, 1540−1550.
(19) Raval, R.; Parker, S. F.; Pemble, M. E.; Hollins, P.; Pritchard, J.; Chesters, M. A. *Surf. Sci.* **1988**, *203*, 353−377.
(20) Mak, T. C. W. *Z. Kristallogr.* **1984**, *166*, 277−281.
(21) Rosa, A.; Baerends, E. J.; van Gisbergen, S. J. A.; van Lenthe, E.; Groeneveld, J. A.; Snijders, G. *J. Am. Chem. Soc.* **1999**, *121*, 10356−10365.

(22) Rolke, J.; Zheng, Y.; Brion, C. E.; Charkavorty, S. J.; Davidson, E. R.; McCarthy, I. E. *Chem. Phys.* **1997**, *215*, 191−205.
(23) http://webbook.nist.gov.
(24) Lee, K.; Morikawa, Y.; Langreth, D. C. *Phys. Rev. B* **2010**, *82*, 155461.
(25) Vosegaard, T.; Skibsted, J.; Jakobsen, H. J. *J. Phys. Chem. A* **1999**, *103*, 9144−9149.